# SEISMIC PERFORMANCE OF BUTTERFLY SHAPED SLIT DAMPERS WITH VARYING SLIT ANGLES

**Dip Narayan Yadav[1*], Md. Basir Zisan[2], Shakwat Karim Maher[3], Fahim Shahriar[4],**

[1*]*Graduate student, Department of Civil Engineering, CUET, Bangladesh, e-mail: dipyadav79@gmail.com*
[2]*Professor, Department of Civil Engineering, CUET, Bangladesh, e-mail: basirzisan@cuet.ac.bd*
[3]*Research Assistant, Department of Civil Engineering, CUET, Bangladesh, e-mail: shakwatkarim8880@gmail.com*
[4]*Lecturer, Department of Civil Engineering, CUET, Bangladesh, e-mail: fahim.shahriar@cuet.ac.bd*

***Corresponding Author**

## ABSTRACT

In recent times, the incidence of earthquakes has been increasing day by day and it is causing great damage to people's lives, structures, infrastructure and economic activities. In such circumstances, the use of slit dampers as an energy dissipation device in earthquake-resistant steel structures has become important, as they protect the structure by absorbing the effects of vibration and providing controlled plastic deformation under repetitive loads. However, conventional slit dampers are often designed with narrow slits, which results in reduced damper flexibility and fatigue resistance due to high stress concentration at the ends of the slits. To solve this problem, this study analyzed the effect of butterfly-shaped slit dampers, in which the slit is narrower in the middle and wider at the sides, helping to distribute the stress more evenly. For the study, nonlinear finite element models with six different slit angles 90°, 85°, 80°, 70°, 60°, and 50° were prepared using the multi-linear kinematic hardening properties of mild steel, in which the 90° model represents a conventional simple slit. Repeated seismic effects are simulated by applying gradual displacement controlled loading to each model, and the mesh, boundary conditions and other modeling settings are carefully checked to ensure realistic results. The analysis showed that at small slit angles, plastic deformation is mainly concentrated in the middle part of the slit, which increases the initial stiffness, strength, and maximum load capacity, but reduces flexibility; Larger slit angles make the damper more flexible, but reduce force capacity. Energy dissipation was found to be best at mid-level angles, and the 70° slit in particular showed the best balance of strength, flexibility, and hysteresis energy dissipation. Therefore, the 70° butterfly slit damper is suitable for controlling both force and deformation in seismic design, and the results of this study provide practical guidance on the size selection of such dampers in steel structures, which help to protect the building under repeated seismic loads and improve long-term performance.

***Keywords:*** *Butterfly slit damper, Slit angle, Energy dissipation, Passive control, Seismic performance*

## 1. INTRODUCTION

Earthquakes are very dangerous to buildings and in a bid to ensure that structures are safe against seismic events, various instruments with the potential to absorb and release seismic energy are used. The most common of these are passive energy dissipation devices, which can achieve this objective because they can undergo controlled inelastic deformations during an earthquake to relieve structural damage (Soong & Dargush, 1997). Metallic yield dampers are the most popular since their hysteretic behavior is constant, reliable, and economical.

A typical metallic damper is known as a steel slit damper. They are made by cutting holes into a steel plate, forming several vertical strips which are flexural links. These strips become strain gauges when exposed to lateral forces, dissipating seismic energy by means of plastic deformation (Oh et al., 2009). Such beneficial features of slit dampers are their small size, high energy dissipation, and easily replaceable in the post-major seismic event, with concentrated damage not on the primary members of the structure (Lee et al., 2017).

However, traditional slit dampers that have straight parallel strips can experience stress concentration at the end of the slits, which can lead to premature fracture and a steep decrease in strength (Lee et al., 2015). In order to overcome this drawback, different geometric adjustments have been studied by researchers. As an example, tapered strip dampers have been designed to distribute plasticity more directly around the height of the strip, enhancing ductility and energy dissipation (Lee et al., 2016). According to this concept of geometric optimization, the butterfly-shaped slit damper has become an effective tendency. This design incorporates slits that have curved, hourglass-shaped profile, and this aspect seeks to distribute stress more equally, increase stability during cyclic performance as well as postponing the initiation of local buckling or tearing.

Although the rudimentary notion of shaped slit dampers appears to have some potential, the interaction between the geometric parameters, in particular, and their functionality remains poorly understood. The results of comparative studies conducted recently have brought to the fore the fact that the material properties and cyclic loading protocols of slit dampers have considerable impact on hysteretic response (Hwang et al., 2022). Nevertheless, limited studies have been conducted to focus on the most important parameter that needs to be studied in butterfly-shaped designs, namely slit angle, and its direct influence on the main performance indicators (Farzampour & Eatherton, 2019).

So, this paper conducts research on the seismic behavior of the butterfly shaped slit dampers under the finite element method (FEM). The geometry of the damper is kept constant, the slit angle was varied to 50°, 60°, 70°, 80°, 85° and 90°. The aim is to assess the effect that this angle has on the initial stiffness, yield strength, maximum load capacity, hysteretic stability, effective damping, and ductility of the damper at cyclic load. The results will be useful in the optimization of butterfly-shaped slit dampers design to improve seismic protection.

## 2. METHODOLOGY

### 2.1 Geometry of Slit Dampers

In Figure 1, six angular steel damper setups with angles of 90°, 85°, 80°, 70°, 60°, and 50° along with their geometric measurements, all of which are in millimetres, are shown. The figures also denote the type of damper model as "BD-X" where BD is used to represent the butterfly damper and X is the slit angle. The damper is 10 mm thick and has five openings, or slits. The height of each damper is 140 mm and the width is is variable; however, the cross-sectional area at section A-A is identical for all the damper models. At the section level A-A, the slits are separated with links that are 20 mm wide.

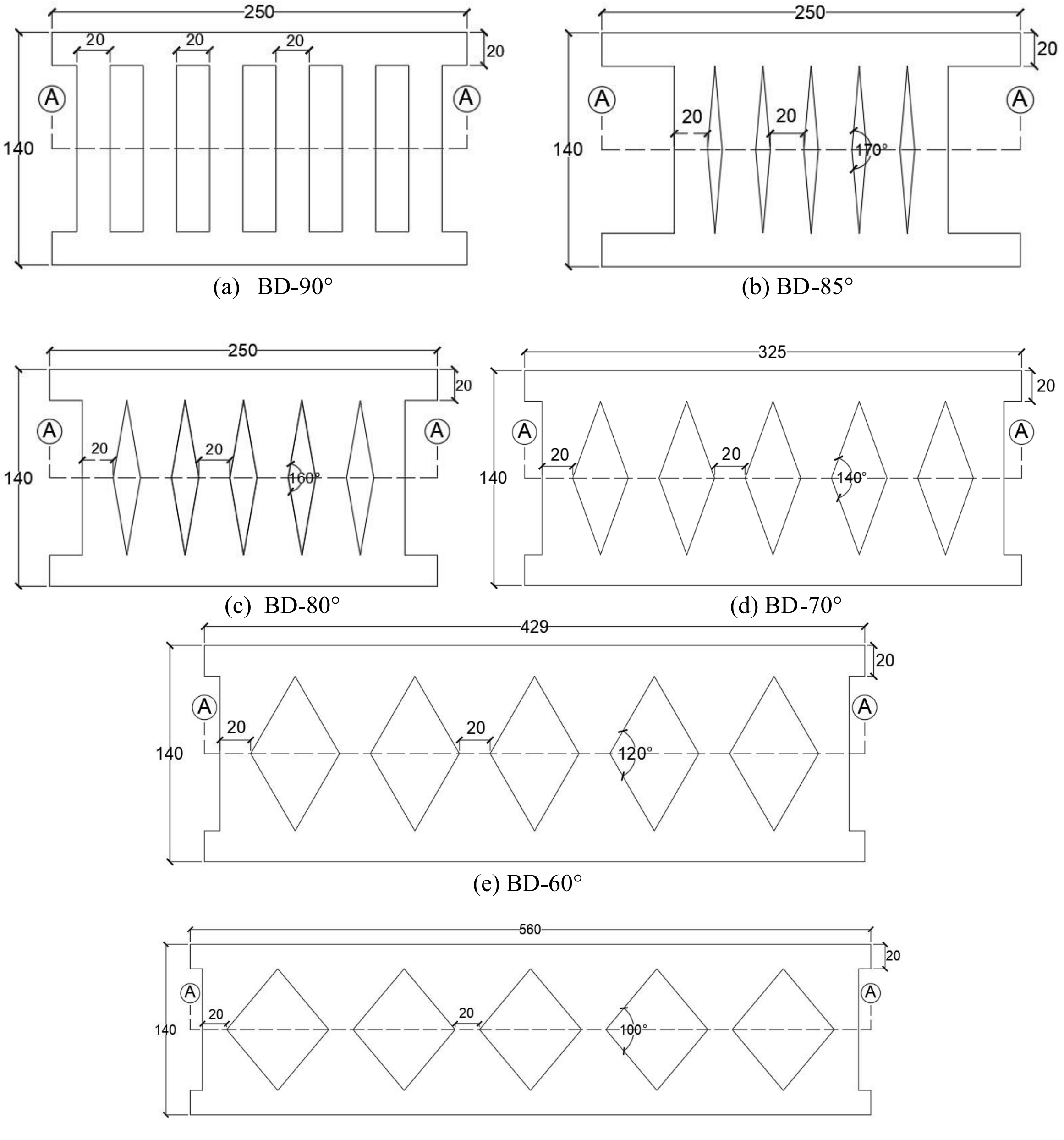


(a) BD-90° (b) BD-85°

(c) BD-80° (d) BD-70°

(e) BD-60°

(f) BD-50°

Figure 1: The detailed dimensions of each damper.

## 2.2 Finite Element Modelling

A numerical analysis using ANSYS based on the finite element method was done to explore the behaviour of steel slit dampers with different slit arrangements under seismic loading. All the models were put under the same boundary conditions and were equal in geometric properties in order to achieve uniformity and comparability. The damper models were discretized using two-dimensional solid elements, with a refined mesh density implemented in regions proximate to the slit tips and connection interfaces to precisely represent localized inelastic deformation and stress intensification phenomena. The constitutive response of the steel dampers was defined by an elastic-plastic material model incorporating a Voce-type nonlinear isotropic hardening law. The material parameters and data for the Voce-type nonlinear isotropic hardening law are presented in Table 1.

Table 1. Summary of material parameters

| | | |
|---|---|---|
| Isotropic Hardening | Density, D (kg.mm$^{-3}$) | 7850 |
| | Young's modulus of elasticity, E (GPa) | 200 |
| | Poison's ratio, $\mu$ | 0.3 |
| | Yield stress, $F_y$ (MPa) | 295 |
| Nonlinear Isotropic Hardening Voce Law | Initial Yield stress $\sigma_0$ (MPa) | 295 |
| | Linear hardening coefficient, $H_{lin}$ (MPa) | 16 |
| | Exponential hardening coefficient, $Q_{exp}$ (MPa) | 30 |
| | Exponential saturation parameter, b | 50 |

## 2.3 Finite Model Verification

For the model verification, specimen PSD-5, as shown in Figure 2(a) was taken from Shah and Moradi (2020). The specimen has a length of 210 mm, a width of 460 mm, and a thickness of 10 mm. The vertical slits have a length of 180 mm and a width of 10 mm. These vertical slits are separated by straight links 36 mm wide. The boundary conditions assumed in the FE analysis are assumed to be similar to those of the experimental study as given in Teh, Tan, Chan, and Rotter (2015). The bottom part of the damper is fully fixed, meaning that all translational and rotational degrees of freedom are restricted. The opposite upper part of the damper is subjected to displacement-controlled cyclic loading applied in the lateral direction along the x-axis. There is no vertical compression load on the damper. The loading protocol is shown in Figure 2(b). This loading procedure follows the same loading pattern that was used by Teh et al., (2015).

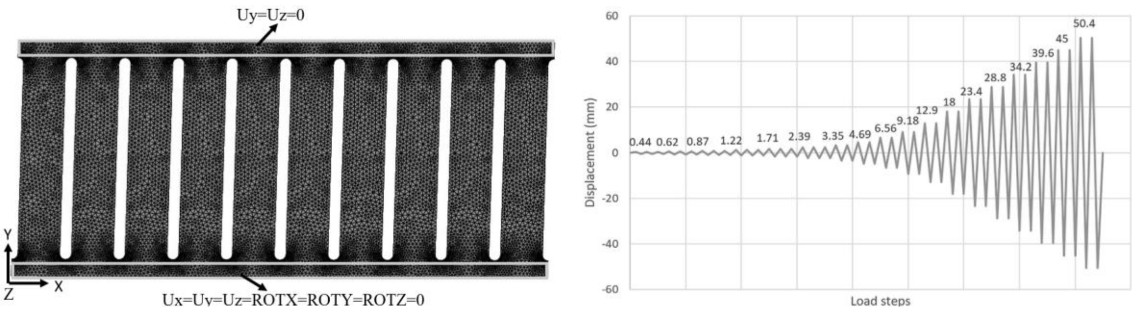


(a) Boundary conditions (b) Cyclic loading history

Figure 2: Boundary conditions and cyclic loading history (Shah & Moradi, 2020; Teh et al. 2015)

The finite element model was validated through a comparison of hysteresis curves between FE analysis and experimental study performed by Shah and Moradi (2020) and Teh et al. (2015). Figure 3 shows the comparison of hysteresis curves. It is seen that the FE model is capable of accurately reproducing the response of the damper that is observed in the experiment, with a minimal percentage error. Therefore, the FE model is assumed to be accurate for further investigations.

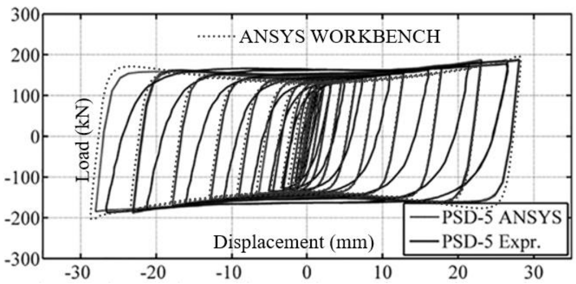


Figure 3: FE model validation

## 3. RESULTS

### 3.1 Hysteretic and Skeleton Curves

Figure 4 illustrates the hysteretic behavior of butterfly-shaped steel dampers with varying slit angles, ranging from 50° to 90°. The loops of hysteresis observed show that there is a strong correlation between slit angle and loop shape and width. This difference implies that the energy dissipation and deformation capabilities are different. Dampers that have a larger slit angle (80°–90°) have larger hysteresis loops and greater displacement potential, which implies greater ductility and energy absorption potential. Conversely, smaller slit angles (50°–60°) exhibit smaller loops, indicating lower deformation capacity and reduced effectiveness in dissipating energy.

The calculated values have shown that the maximum resisting force values were 99.23 kN, 136.43 kN, 156.80 kN, 239.03 kN, 310.38 kN and 332.73 kN and the corresponding maximum displacements at the failure level were 28.8 mm, 28 mm, 23.4 mm, 18 mm, 18 mm, and 9.18 mm of dampers with slit angles of 90°, 85°, 80°, 70°, 60°, and 50°, respectively, as shown in Fig. 5. These findings indicate that the displacement that the damper maintains at the failure level decreases with the reduction of the inclination of the slit edges at level A-A. The 90° damper showed the most displacement of 28.8 mm and 50° damper had the least displacement of 9.18 mm. As a result, the greater the slit angle augmented, the greater the deformation capacity of the damper. This enhanced deformability increases the extent to which the structural element can undergo a greater number of cycles before structural failure, thus improving the overall seismic energy dissipation performance of the component.

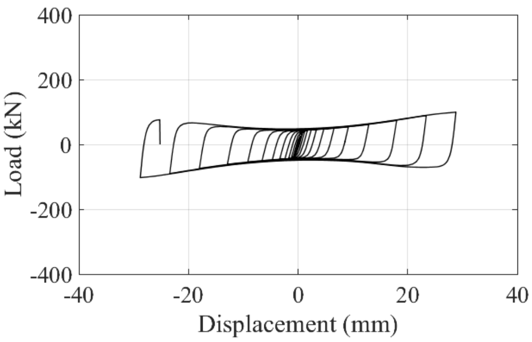


(a) BD-90°

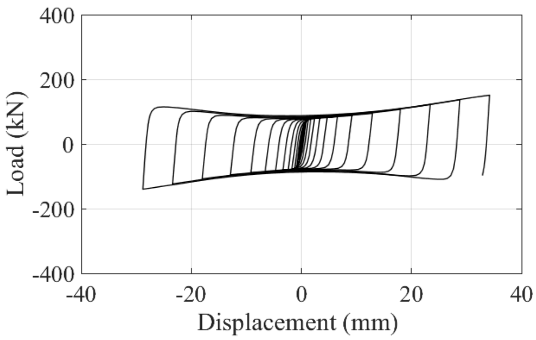


(b) BD-85°

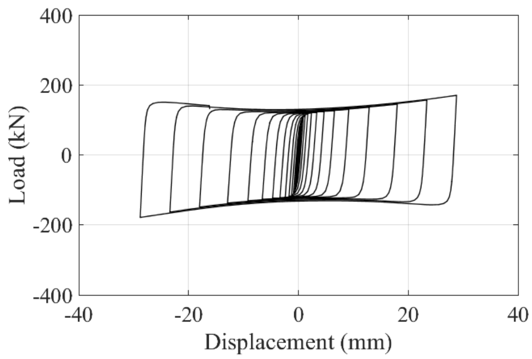


(c) BD-80°

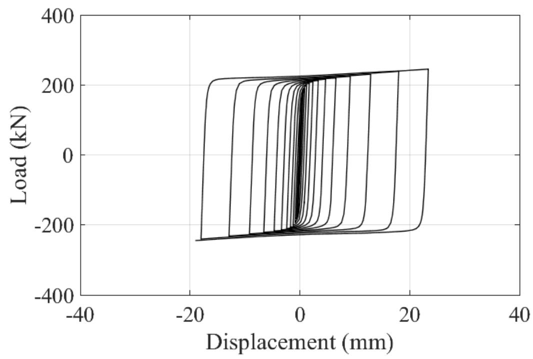


(d) BD-70°

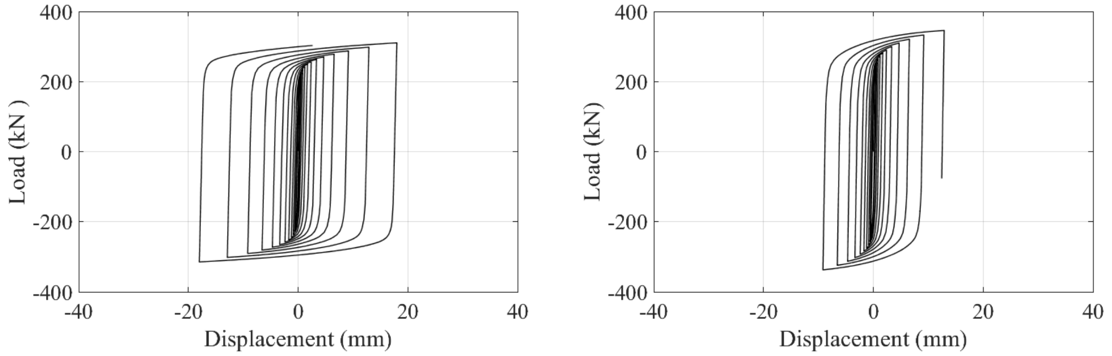


(e) BD-60° (f) BD-50°

Figure 4: The hysteretic curves of each damper.

The figure 5 illustrates the respective skeleton curves, which have been drawn with the interconnection of the peak points of each hysteresis cycle. The skeleton curves, symbolizing envelope of hysteretic responses of butterfly dampers with slit angles varying between 90° and 50°, show a clear tendency of the structural behavior as the slit angle narrows. Normal nonlinear behavior is exhibited by all the specimens, with an initial linear-elastic phase followed by yielding, peak load and a post-peak softening. It is important to note that the reduction in the slit angle (90° to 50°) results in a very drastic increase in the maximum load carrying capacity of 99.23 kN to 332.70 kN and the displacement at peak loading also drastic increase. This inverted strength-deformation relationship indicates that, in effect, the failure mode is changed: the larger the angle of the damper, the more ductile and displacement-controlled is the damper, and the smaller the angle, the stronger the damper is and the less it will deform before failure.

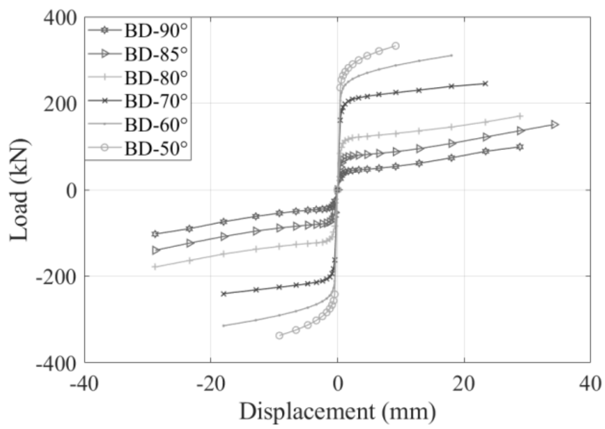


Figure 5: The skeleton curves of each damper.

### 3.2 Behaviour of Damper Under Cyclic Load

Figure 6 shows von Mises stress distributions of slit dampers of butterfly shape with different angles of slits of 50° to 90°. These stress contours are plotted at a displacement level of 9.18 mm and time 20 s as shown in Fig. 6. The damper material has a yield strength of 295 MPa. The regions exhibiting the stress levels exceeding 295 MPa, indicated by darker shading, signify the onset and development of plastic deformation. Study of these contours shows that as the slit angle decreases; the plastic deformation moves toward the apex of the angle at damper center.

Stress distributions analysis shows that there is a direct relationship between decreasing slit angle and increasing maximum stress. Maximum stress increased from 352.63 MPa at 90° to 422.23 MPa at 50°. The increased stress levels at higher slit angles (85°- 90°) were mainly concentrated at the outer edges of the slit, and thus indicate that they began yielding first at the outer edges of the slit. On the other hand, plastic areas increased in size and spread to the centre of the apex of the damper at low slit angles especially at 60° and 50°. This action is an indication that the smaller the slit angles, the greater the concentration of stress and the power of dissipation in the middle of the damper, which may compromise global ductility.

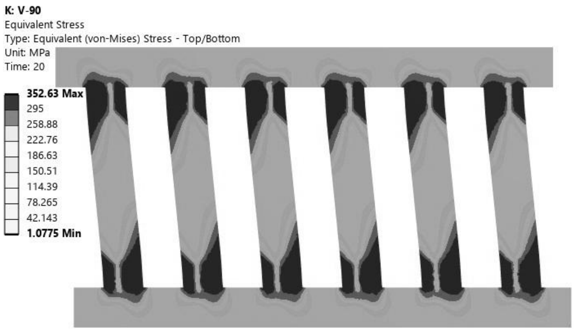


(a) BD-90°

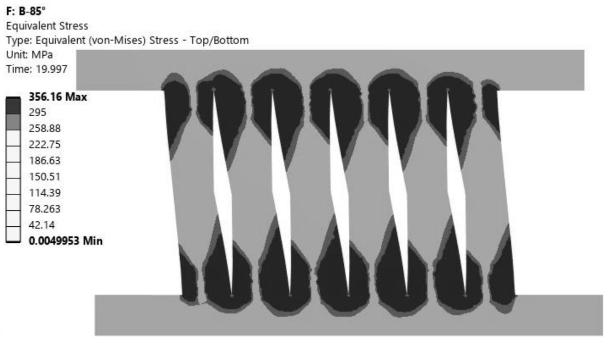


(b) BD-85°

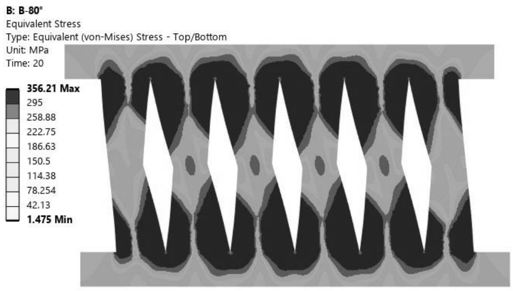


(c) BD-80°

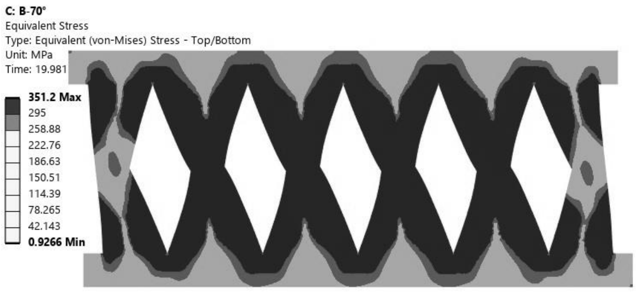


(d) BD-70°

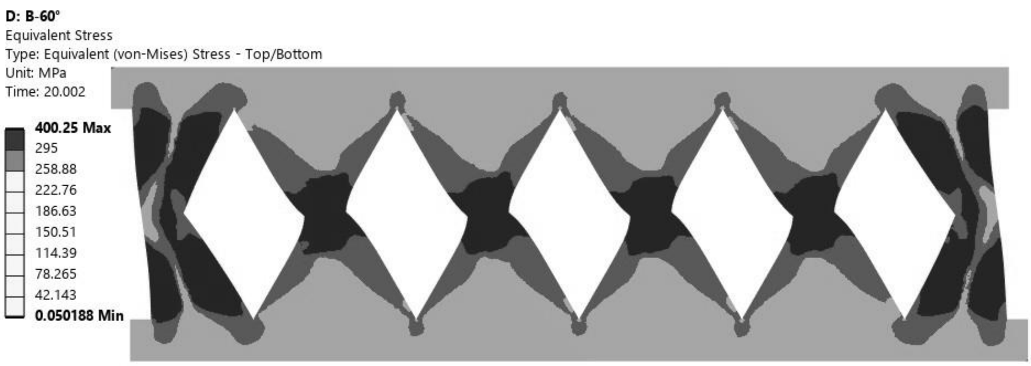


(e) BD-60°

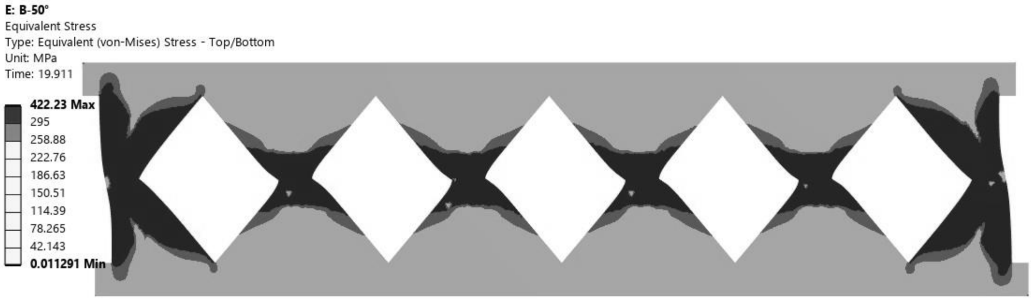


(f) BD-50°

Figure 6: Stress contours for each damper.

### 3.3 Energy Dissipation

The cumulative area of hysteresis loops at various displacement levels measured provides a measure of energy dissipation as illustrated in Fig. 7. The graph is used to compare the magnitude of energy taken by each damper at various displacements. The findings show that the energy dissipation proportional to displacement increases with the displacement, a characteristic of the conventional hysteretic action of metallic dampers during periodic loading. The effective energy lost and the displacement of the same are, however, largely dependent on the slit angle.

The most efficient energy absorption damper is the 60° damper since it is able to absorb the highest amount of energy, approximately 20,303 kN.mm at a displacement of 18 mm. Next there are the 70° and 80° which, had values of 15,663 and 12,259 kN·mm, respectively. This implies that middle slit angles provide a compromise between stiffness and ductility. The 85° damper presents 11,289 kN.mm at 28 mm and the 90° which has the greatest deformation (28.8 mm), only dissipates 5,833 kN·mm. This implies that larger slit angles are less efficient.

The capacity of the energy dissipation is higher with the slit angle being reduced to 60 degree. This is because the distribution of the plastic stress and deformation in damper is optimized. But when the angle gets too small, as 50°, the deformation stays in one place, and the energy absorption goes down. So, the 60° slit angle gives the best balance of strength, ductility, and ability to absorb energy.

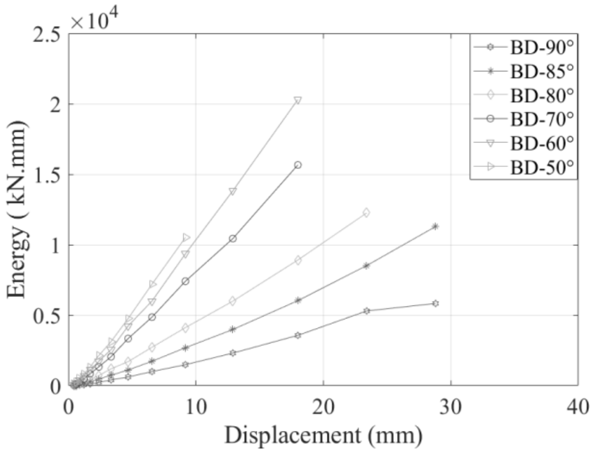


Figure 7: The energy dissipation of each damper.

### 3.4 Analysis of Response Characteristics for Damper

Based on the cyclic loading and skeleton curves as given in Fig. 5, six key parameters for the steel damper were determined: initial stiffness ($K$), yield strength ($P_y$), ultimate stiffness, effective damping ($\beta_{eff}$), maximum strength ($P_{max}$) and ductility ($\mu$). The initial stiffness is defined as the ratio of yield strength to yield displacement, while the ultimate stiffness is calculated from the slope of the final segment of the load displacement curve. Ductility is defined as the ratio of the maximum displacement to the yield displacement. The maximum load represents the peak strength of the damper, whereas the yield strength corresponds to the load at the onset of yielding.

In particular, effective stiffness and damping provide a measure of the damper's ability to absorb and dissipate energy under cyclic loading. The effective stiffness ($K_{eff}$) is calculated using Eq. (1).

$$k_{eff} = \frac{|P^+ + P^-|}{|\delta^+ + \delta^-|} \quad (1)$$

where $\delta^+$ and $\delta^-$ are the peak displacements in positive and negative directions and $P^+$ and $P^-$ their corresponding peak loads, respectively. The effective damping ratio ($\beta_{eff}$) is determined using Eq. (2).

$$\beta_{eff} = \left(\frac{2}{\pi}\right)\frac{E_{loop}}{k_{eff}(|\delta^+| + |\delta^-|)^2} \quad (2)$$

Here, $E_{loop}$ represents the area of the hysteresis loop. These above mentioned parameters are commonly used in cyclic tests to measure how stiffness decreases and how much energy the damper can absorb. A comparison of these properties for the different steel dampers is summarized in Table 2.

Table 2. Response characteristics of each damper

| **Model** | **Initial Stiffness (kN/mm)** | **Yield Strength (kN/mm)** | **Ultimate Stiffness (kN/mm)** | **Effective Damping** | **Maximum Strength (kN)** | **Ductility** |
|---|---|---|---|---|---|---|
| BD-90° | 39.813 | 27.17 | 1.91 | 0.32 | 99.23 | 27.80 |
| BD-85° | 74.183 | 53 | 4.95 | 0.451 | 136.43 | 64 |
| BD-80° | 117.03 | 80 | 2.51 | 0.521 | 156.80 | 63.16 |
| BD-70° | 208.63 | 164 | 1.69 | 0.578 | 239 | 40 |
| BD-60° | 252.96 | 210 | 2.43 | 0.575 | 310 | 40 |
| BD-50° | 270.83 | 274 | 4.61 | 0.54 | 332 | 64 |

The initial stiffness value was significantly higher at smaller slit angles, rising from 39.81 kN/mm at 90° to 270.83 kN/mm at 50°. This tendency suggests that smaller slit angles offer increased resistance to deformation at the first loading stage which, can be explained by better material continuity and reduced stress concentration along the slit area.

The same trend was observed with yield strength and ultimate strength, which both had a significant increase with a reduction in the slit angle. The highest ultimate strength was observed in the BD-50° configuration which was, at 332 kN, confirming its increased load-bearing capacity compared to dampers with larger slit angles. However, the increase in strength was associated with the decrease in ductility in some samples. In particular, the deformation capacity of BD-70° and BD-60° were smaller than those of BD-85° and BD-50°, indicating that there is an inverse relationship between strength and ductility and it depends on the slit geometry.

Across the examined arrangements, the BD-70° variant showed the highest effective damping ratio (0.578), indicating enhanced energy dissipation under repeated loading. While BD-60° and BD-50° also demonstrated **considerable resistance**, their damping capabilities were marginally inferior to those of the BD-70° configuration. Overall, the BD-70° design provided the best tradeoff between rigidity, resistance and energy dissipation, which may provide a valuable design in seismic applications where load-bearing capacity, as well as controlled deformation is important.

## 4. CONCLUSIONS

This study examines how the seismic behavior of butterfly-shaped dampers is influenced by changes in slit angle. In particular, the research will seek to clarify how geometric modification and stress distribution, energy dissipation potential, stiffness properties, and the general behavior of hysteretic response to cyclic loading are related. Simulation of cyclic loading conditions through displacement control described the condition of dampers through finite element analysis, and the data obtained were compared at slit angles of 50° and 90°. The objective is to determine a configuration that effectively balances strength, ductility, and energy dissipation for enhanced seismic resistance.

Based on the analytical study, the following conclusions are founded:

i. The analysis of the stress contours showed that the plastic deformation shifted to the edges of the slit (at larger angles) to the central apex (at smaller angles). This implies a high concentration of stress and increased dissipation of energy with a reduction in the slit angle.
ii. The maximum energy dissipation was increased by decreasing slit angle; the 60° configuration showed the highest cumulative hysteretic energy, indicating an optimum balance between stiffness and deformation capability.
iii. Initial stiffness, yield strength and maximum strength were all higher with smaller slit angle, indicating an increased load-bearing capacity of dampers with small slit angles.
iv. A negative correlation was found between stiffness/strength and ductility: lower slit angles led to higher levels of stiffness and strength with lower ductility, and higher levels of ductility with lower strength and energy dissipation.
v. The 70° slit geometry was found to have the best compromise of stiffness, energy dissipation and ductility. This feature renders it applicable in seismic applications where the load capacity and deformation is to be regulated.
vi. The results provide guidance for performance-based design methodologies in selecting and optimizing steel dampers for earthquake-resistant structures.

The current scope of this investigation and its findings are limited to finite element analysis only. Future research endeavors should encompass empirical validation via experimental testing and comprehensive, full-scale structural substantiation to corroborate the performance patterns discerned in the simulations.

## REFERENCES:

Farzampour, A., & Eatherton, M. R. (2019). Parametric computational study on butterfly-shaped hysteretic dampers. *Frontiers of Structural and Civil Engineering, 13*(5), 1214–1226.

Hwang, S. J., Lee, D. H., & Kim, Y. J. (2022). Comparative study on hysteretic behavior of steel slit dampers under cyclic loading protocols. *Journal of Constructional Steel Research, 192*, 107229.

Lee, C. H., Kim, H. J., & Min, K. W. (2015). Cyclic behavior and fracture characteristics of slit steel dampers. *Engineering Structures, 99*, 192–204.

Lee, C. H., Kim, H. J., Min, K. W., & Kang, S. M. (2016). Seismic performance of steel slit dampers with tapered links. *Journal of Constructional Steel Research, 121*, 92–104.

Lee, C. H., Min, K. W., Kim, H. J., & Kang, S. M. (2017). Experimental and numerical study on replaceable steel slit dampers for seismic energy dissipation. *Steel and Composite Structures, 25*(4), 411–423.

Oh, S. H., Kim, Y. J., & Ryu, H. S. (2009). Seismic performance of steel slit dampers fabricated with low-yield-point steel. *Engineering Structures, 31*(2), 512–521.

Shah, K., & Moradi, S. (2020). Numerical and experimental investigation of perforated steel plate shear walls for energy dissipation. *Engineering Structures, 213*, 110589.

Soong, T. T., & Dargush, G. F. (1997). *Passive energy dissipation systems in structural engineering*. John Wiley & Sons.

Teh, L. H., Tan, J. S., Chan, R. W. K., & Rotter, J. M. (2015). Yielding shear panel device for passive energy dissipation. *Engineering Structures, 87*, 42–52.